Evolution of Structure in CH_5^+ and Its Deuterated Analogues

Lindsay M. Johnson and Anne B. McCoy*

Department of Chemistry, The Ohio State University, Columbus, Ohio 43210

Received: March 17, 2006; In Final Form: May 14, 2006

Diffusion Monte Carlo simulations are used to investigate the effects of deuteration on the fluxionality of CH_5^+ or CD_5^+, using an ab initio potential surface, developed by Jin, Braams, and Bowman [*J. Phys. Chem.* **2006**, *110*, 1569]. We find that partial deuteration quenches the fluxional behavior. The spectral consequences are also investigated. We find that, while CH_5^+ and CD_5^+ are nearly spherical tops, partial deuteration breaks the rotational symmetry and the mixed isotopologues are generally better characterized as symmetric tops. In addition, we investigate the effects of deuteration on the low-resolution vibrational spectrum and anticipate that signatures of this delocalization will be observable in the vibrational spectrum.

1. Introduction

The carbonium ion, CH_5^+, has been a system of long-standing interest due to its importance as an intermediate in reactions in the interstellar medium[1] and in combustion chemistry. It is also the simplest of Olah's hypercoordinate carbocations.[2] From a more fundamental perspective, CH_5^+ has intrigued a number of workers as the addition of a proton to CH_4 takes a rigid methane molecule and turns it into a highly fluxional species. This has been borne out in quasi-classical studies,[3] ab initio path integral studies,[4−7] as well as diffusion Monte Carlo investigations.[8−10] In fact, the zero-point energy in CH_5^+ provides more than enough energy along the isomerization coordinates to allow for the exchange of any pair of identical nuclei. This has led to interest in CH_5^+ from a group theoretical perspective.[11−13] It has also made the assignment of the high resolution spectrum particularly challenging.[14,15]

As noted above, CH_5^+ is a highly fluxional molecule. This behavior can be attributed to the existence of three low-lying stationary points on the potential surface. These are illustrated in Figure 1. The global minimum has C_s symmetry and is labeled C_s(I) in Figure 1. In this structure, the hydrogen atoms that are labeled a and b are separated by 1 Å. In addition, the distance between these two hydrogen atoms and the central carbon atom are roughly 0.1 Å larger than the other three CH distances.[16−18] The bonding associated with the C, H_a, and H_b interaction has been characterized as a three-centered, two-electron bond. As such, the frequencies that are associated with these two CH stretching vibrations in CH_5^+ are much lower than a typical CH stretch vibration. The hydrogen atom that is labeled *c* in the C_s(I) structure is in the same plane as the carbon atom and the hydrogen atoms labeled a and b, while H_d and H_e lie above and below this plane. The harmonic CH stretch frequencies associated with these three hydrogen atoms are $\geq$3000 cm^{-1}, frequencies that are characteristic of CH stretch vibrations.

The lowest energy saddle point on the CH_5^+ potential surface is roughly 30 cm^{-1} above the global minimum.[18] It also has C_s symmetry and is identified as the C_s(II) stationary point. Comparing the C_s(I) and C_s(II) structures in Figure 1, we find that they are related by a 30° rotation of the CH_3^+ unit so that H_c is no longer in the plane that contains the carbon atom, H_a and H_b. A second low energy stationary point that we will consider is the one with C_{2v} symmetry that lies approximately 340 cm^{-1} above the global minimum.[18] Motion across this saddle point corresponds to motion of H_b between H_a and H_c.

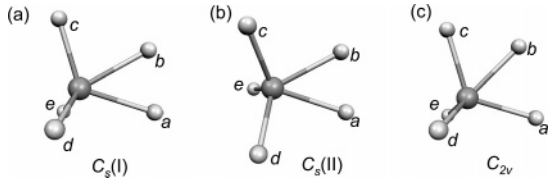

Figure 1. Three structures of CH_5^+ at (a) the global minimum [C_s(I)], (b) the saddle point for rotation of the CH_3^+ group [C_s(II)], and (c) the saddle point for the flip isomerization [C_{2v}].

Interestingly, when the harmonic zero point energy is added to the electronic energy at each of the stationary points, the energy ordering is reversed, with the C_{2v} saddle point becoming the lowest energy structure and the C_s(I) structure having the highest energy. The differences among the energies of the stationary points are smaller than 30 cm^{-1}, and anharmonic effects are likely to change the ordering.[19] This simple calculation indicates that when the differences in the CH stretch and HCH bend frequencies at the three stationary points in Figure 1 are taken into account, the effective potential is flat along the two coordinates that correspond to exchanging the labels of identical hydrogen atoms.

An interesting question arises as to what happens if the symmetry of the system is broken, either through partial deuteration, or by forming complexes with H_2, as was done in studies of Lee and co-workers.[20,21] In these studies, Boo et al. found that the spectrum in the CH stretch region changes with the introduction of one to three H_2 molecules, but when it is complexed with three or more hydrogen molecules, only small changes to the spectrum were observed. Likewise, Marx and Parrinello investigated CH_4D^+ and CHD_4^+ by path integral Monte Carlo methods in order to shed light on the apparent contradiction between the highly fluxional behavior, outlined above, and the experimental findings of Nibberling and co-workers, which indicated structural preferences in the partially deuterated isotopologues.[6,22] In that work, they found that partial deuteration breaks the symmetry of CH_5^+ by rendering the various potential minima inequivalent once zero-point energy

* E-mail: mccoy@chemistry.ohio-state.edu.

10.1021/jp061675c CCC: $33.50
Published on Web 06/10/2006

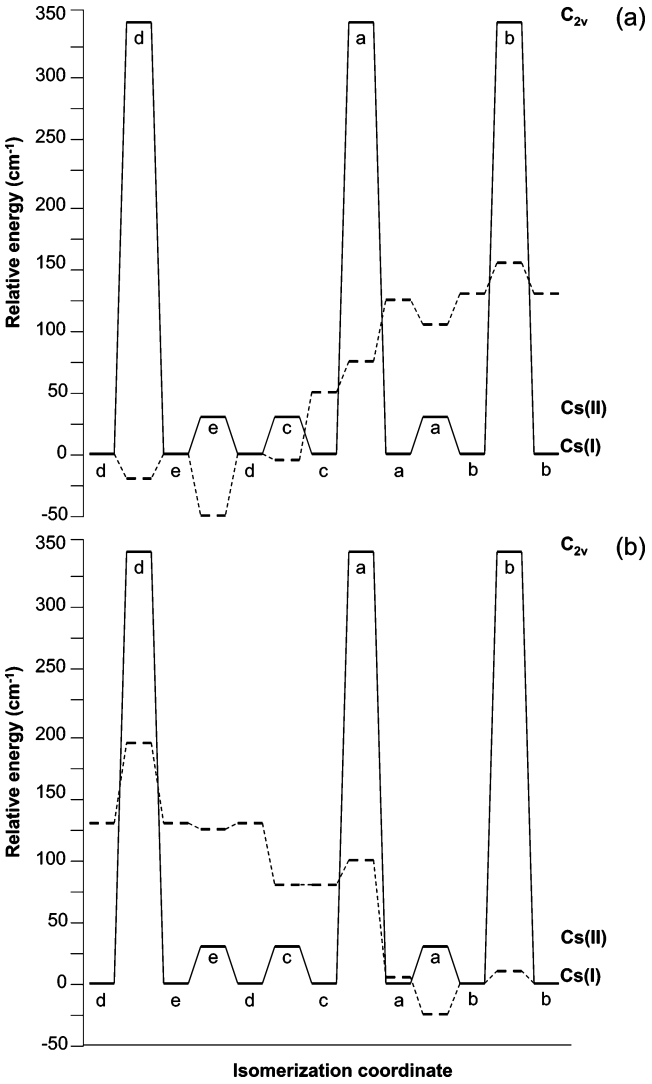

Figure 2. Electronic energies (solid lines) and the sum of the electronic energies and harmonic zero-point energies (dashed lines) along the isomerization paths for (a) CH_4D^+ and (b) CHD_4^+. The letters provide the location of the deuterium atom in panel a and the hydrogen atom in panel b. To facilitate comparison the symmetry labels of the three stationary points are written on the right side of each graph at their corresponding energies.

is considered. While at high temperatures these effects will become less important, at low temperatures they can be important. In the present work, we use diffusion Monte Carlo (DMC) methods to explore these effects. We focus on the question of how deuteration affects the free exchange of the hydrogen or deuterium atoms. In addition, we explore the consequences of the quenching of the fluxional behavior of CH_5^+ on the vibrational spectrum of its isotopologues.

2. System

As noted above, CH_5^+ is a highly fluxional molecule. It has 120 equivalent minima. More importantly, the saddle points that interconnect these minima have roughly the same energy as the minima, once zero-point energy is taken into account.[9,19] On the basis of the same analysis, partial deuteration changes the landscape considerably. In the cases of CH_4D^+ or CHD_4^+, once zero-point energy is considered there are now four energetically inequivalent minima, as shown in Figure 2. This, along with shifts in the energies of the saddle points that connect the minima, leads to more stable structures associated with the single deuterium atom being found in position c, d, or e while the single hydrogen atom is preferentially in position a or b.

Quantification of these effects will require a potential surface and a way to evaluate the wave functions and energies from this potential. During the past 3 years, three ab initio potential surfaces have been reported for CH_5^+. The first was an MP2-based surface by Brown, Braams, and Bowman.[9] This surface is a high-order polynomial fit to more than 20 000 electronic energies and a larger set of gradients, obtained at the MP2/cc-pVTZ level of theory/basis. The majority of the geometries at which the electronic energies were calculated came from direct dynamics simulations, run over a range of energies using MOLPRO. These points were augmented by points that were chosen from the grids that are used for their MULTIMODE program.[23] The functions that were used for the fits were permutationally invariant polynomials, based on functions of the atom−atom distances. More recently, the energies at these geometries were reevaluated at the CCSD(T)/aug-cc-pVTZ level of theory/basis and the resulting points were refit by Jin, Braams, and Bowman. This is the surface that has been used in the present work. Jin et al. extended this surface so that it extrapolates to the correct dissociation limits and have performed calculations of the ground-state energy using diffusion Monte Carlo (DMC) for all six isotopologues.[18] These will be compared with the present results. A third potential surface was developed independently by Thompson, Crittenden, and Jordan.[10] This surface is based on electronic energies and Hessians, evaluated at the CCSD(T)/aug′-cc-pVTZ level of theory/basis using GAUSSIAN 98. In contrast to the fits of Bowman and co-workers, this potential is constructed using the Shephard interpolation, within the GROW 2.2 package of Collins and co-workers. To construct this potential, Thompson et al. used DMC to determine where additional points would be needed and based the final surface on 179 electronic energies and Hessians.

The second ingredient for being able to investigate CH_5^+ is a method that can be used to obtain vibrational energies and wave functions. At present, our focus is on ground state properties. As such, an ideally suited approach is diffusion Monte Carlo. For excited states, Huang and Bowman have used vibrational configuration interaction (VCI) approaches, as implemented in the program MULTIMODE, to study these species with excellent success.[15,24]

3. Coordinates and Hamiltonian

Having elected to employ diffusion Monte Carlo (DMC) approaches for this study, we use the 3*N* Cartesian coordinates that define the system, and, consequently the Hamiltonian is expressed in these coordinates. While this choice leads to a simple form for the kinetic energy operator, the analysis of the wave function requires the introduction of an embedding of the body-fixed axis system and the introduction of several internal coordinates.

In DMC we obtain an ensemble of replicas that provide a Monte Carlo sampling of the ground-state wave function for CH_5^+. To define internal coordinates, we need to put labels onto the five hydrogen atoms. When we start the simulation, each of the hydrogen atoms is in a distinct bonding site. As the molecule is allowed to sample the potential surface, each of the hydrogen atoms will sample all five possible bonding sites, labeled a−e in Figure 1. At all three stationary points, the H_a−H_b distance is smaller than or equal to the other nine HH distances. Consequently, we label the two hydrogen atoms that are closest together with the letters a and b. In addition, the

next shortest HH distance involves the hydrogen atoms in positions b and c. We use these constraints to assign these labels. The remaining two hydrogen atoms are labeled d and e. Having labeled the five hydrogen atoms, we define $q = r_{bc} - r_{ab}$, where q is always positive. At the C_{2v} saddle point $q = 0$. At the minimum $q = 0.49$ Å, while at the C_s(II) saddle point $q = 0.60$ Å. To obtain ϕ, we first define an axis of rotation, *z*, to lie along the vector that connects the carbon atom to the center of mass of H_c, H_d, and H_e. Next, we define the *x*-axis so that the vector that connects H_a and H_b lies parallel to the *xz* plane. The coordinate ϕ is defined as the rotation of a hydrogen atom in position *c*, *d* or *e* off of the *xz* plane. As such, at a C_s(I) minimum, the three hydrogen atoms will be located either at 0 and ±120° or at ±60 and 180°, while at the C_s(II) saddle point the locations of the three hydrogen atoms will be rotated by 30° from these values. At the C_{2v} saddle point, $\phi = \pm 90°$ and either 0 or 180°.

4. Theory

To investigate the spectroscopic consequences of deuteration of CH_5^+, we use DMC to evaluate the ground-state wave function and, from it, the ground-state probability amplitudes. The details of this approach and our applications to CH_5^+ are presented, in detail, elsewhere.[9,19,24] Here we provide a short summary, along with a brief discussion of the points that are important for the present study.

The DMC method generates a Monte Carlo sampling of the ground-state wave function, where the sampling points are often referred to as walkers. These walkers are propagated in imaginary time $\tau = it$ using the imaginary-time time-dependent Schrödinger equation.[25] Within this approach, the zero-point energy associated with a particular ensemble of walkers is given by

$$W(\tau) = \bar{V}(\tau) - \alpha\frac{N(\tau) - N(0)}{N(0)} \quad (1)$$

where $\bar{V}(\tau)$ is the average of the potential energy over the positions of the walkers at imaginary time τ and $N(0)$ provides the number of walkers in the ensemble at $\tau = 0$, while $N(\tau)$ gives the number of walkers at time τ. For each of the isotopologues, we perform at least five simulations, over which we vary the value of α from 0.1 to 0.01 hartree, and the initial distribution of walkers. In all cases, we set $N(0) = 20\,000$ and $\Delta\tau = 10$, and the simulations are run for at least 20 000 time steps.

To find the probability density from the ground-state wave functions, we use the descendent weighting approach.[26,27] For these simulations we take the final distribution of walkers from one of the runs, described above. We run the simulation for an additional 25 025 time steps. After every 1000 time steps, we sample the wave function and evaluate $|\Psi|^2$ at the position of each of the walkers by counting the number of descendants over 25 time steps. The reported probability amplitudes are obtained by averaging the results from the last 16 wave functions that are sampled by this method.

As any property, for example the average HH distance, should be invariant under exchange of identical particles, this provides an easy way to test whether the simulations are converged. Specifically, we compare the HH, HD, and DD distributions as well as the CH and CD distributions that are obtained by considering each hydrogen or deuterium atom as being unique. If the simulation is not converged, differences between these distributions will be observed. In these cases, we run the descendent weighting simulations for 125 025 time steps, sample the wave functions every 5000 time steps and count the descendants over 25 time steps. In all cases we find that this is sufficient additional time to equilibrate the simulations.

Three spectroscopic properties that are of interest are the vibrational frequencies, the intensities and the rotational constants. We reported a method for using the relative probability amplitudes at the three stationary points, shown in Figure 1, to obtain vibrational spectra for CH_5^+ at both the harmonic level and using single-reference vibrational configuration interaction (VCI) approaches. In that work, we found that we were able to achieve good agreement with the experimental spectra.[15,28] We also applied the approach to probe the effects of deuteration on the vibrational spectra of CH_4D^+, CHD_4^+ and CD_5^+.[24] Here we apply the approach to the remaining two isotopologues of CH_5^+, namely, $CH_3D_2^+$ and $CH_2D_3^+$. The method is identical to that reported in the Supporting Information to ref 24.

In addition, we have evaluated the vibrationally averaged rotational constants for all six isotopologues. Evaluating these constants requires a definition for the embedding of the body-fixed axis system. Given the high degree of fluxionality of CH_5^+, the optimal choice of embedding is not obvious. In our earlier work on CH_5^+ and CD_5^+, we assumed that the ions were spherical tops and evaluated the elements of the inverse moment of inertia tensor in a space-fixed axis system.[9] While this approach works for these cases, the partially deuterated species are not expected to be spherical tops. Following the work of Jordan and co-workers,[10] we employ an Eckart embedding of the body-fixed axis system, as described by Louck and Galbraith.[29] As this algorithm is based on the separation of rotational and vibrational motions of the system as it moves away from a reference geometry, it is not clear that this should be an appropriate choice for a species as fluxional as CH_5^+. To test this, we performed separate calculations at all three stationary points and for all possible locations of the deuterium atoms for each of the isotopologues. As will be discussed in greater detail below, we find that there is little sensitivity of the rotational constants to the choice of this reference geometry, beyond the statistical uncertainties in the simulations. On the basis of this observation, we believe that the Eckart embedding provides a reasonable approach for evaluating rotational constants for CH_5^+ and its isotopologues.

5. Results

5.1. Zero-Point Energies and Localization of the Ground State. To start, we consider the zero-point energies (ZPE) of the six isotopologues. The results that were obtained for $^{12}CH_5^+$ using the CCSD(T) surface are reported in the second to last row in Table 1. In all cases the results represent the averages of at least five runs, and the numbers in parentheses represent one standard deviation about these means. If we use the ZPE for CH_5^+ as a starting point, we find that the addition of one to three deuterium atoms lowers the ZPE by 600 cm^{-1}. The fourth and fifth deuterium atoms each lower the ZPE, but by only 525 cm^{-1}. Similar trends are seen when we compare the ZPE calculated from the MP2[9] or global CCSD(T)[18] surfaces. The harmonic ZPE of the most stable isotopomer of each isotopologue also shows this trend. These trends can be understood in terms of the harmonic frequencies of the five CH stretches, also reported in Table 1, and the ZPE shifted energy level diagrams for CH_4D^+ and CHD_4^+, shown in Figure 2. Specifically, the CH stretch frequencies in CH_5^+ range from 2430 to 3230 cm^{-1}. Adding a single deuterium atom will lower the ZPE, but, as is seen in Figure 2, the extent of this lowering will depend on the

TABLE 1: Zero-Point Energies and CH/D Stretch Frequencies for CH_5^+ and Its Deuterated Isotopologues, Where All Energies Are Reported in cm^{-1} and the Numbers in Parentheses Provide the Uncertainties

system	CH_5^+	CH_4D^+	$CH_3D_2^+$	$CH_2D_3^+$	CHD_4^+	CD_5^+
a,*b*,*c*[a]	H,H,H	H,H,H	H,H,H	H,H,D	D,H,D/H,D,D	D,D,D
ω_e[b], flip	832	773	722	718	714/631	631
ω_e, CH/D	2429	2299	2216	2130	1885/1890	1728
stretches	2710	2442	2406	2241	2164/2130	1943
	3007	2720	2444	2406	2301/2299	2180
	3128	3018	2725	2489	2406/2405	2303
	3226	3178	3022	2745	2572/2595	2405
harmonic[c]	11 339	10 678	10 010	9382	8832/8835	8272
MP2[d]	10975 (5)	10355 (5)	9745 (5)	9158 (15)	8607 (7)	8080 (5)
global[e]	10917 (3)	10300 (6)	9694 (3)	9097 (6)	8563 (3)	8044 (2)
CCSD(T)	10908 (5)	10298 (5)	9690 (5)	9090 (5)	8559 (5)	8039 (5)
^{13}C	10882 (5)	10269 (5)	9659 (5)	9057 (5)	8522 (5)	8004 (5)

[a] Identity of the atoms in the C_s(I) minimum with the lowest harmonic zero-point energy (ZPE). [b] Harmonic frequencies for the flip and five CH/D stretching modes, evaluated at the C_s(I) minimum with the lowest ZPE. Where two minima have ZPE's that differ by less than 5 cm^{-1}, results for both are reported. [c] Harmonic ZPE. [d] DMC ZPE, evaluated using the surface of ref 9. [e] DMC ZPE, from ref 18.

TABLE 2: Fraction of the Probability Amplitude, Located near Each of the Minima in the Mixed H/D Isotopologues of CH_5^+

a, b, and c[a]	CH_4D^+	$CH_3D_2^+$	$CH_2D_3^+$	CHD_4^+
HHH	0.76	0.42		
HHD	0.17	0.39	0.63	
HDH	0.02	0.05	<0.01	
HDD		0.01	0.09	0.35
DHH	0.05	0.13	0.25	
DHD		<0.01	<0.01	0.54
DDH		<0.01	0.02	0.08
DDD			<0.01	0.03

[a] Type of atoms in positions a, b, and c in Figure 1a.

location of the deuterium atom. As the highest frequency CH stretch vibrations at the C_s(I) minimum energy structure correspond to the symmetric and antisymmetric stretches of the CH_d and CH_e bonds, deuterating in these positions will lead to the greatest lowering of the ZPE. In contrast, the two lowest frequency CH stretch modes correspond to vibrations involving H_a and H_b. As such, in CHD_4^+, the lowest energy structures, when ZPE is considered, are the ones in which the hydrogen atom is in position a or b. The nonlinear decrease in the ZPE with the addition of deuterium atoms provides a first hint that the delocalization of the atoms is partially quenched by deuteration.

To further investigate this quenching of the fluxionality of CH_5^+ upon deuteration, probability amplitudes are binned according to the closest minimum energy structures. The results are reported in Table 2. As positions d and e are equivalent in the equilibrium configuration, we only consider the identity of the atoms (hydrogen or deuterium) in bonding sites a−c in Figure 1. If there were no differentiation between the energies of the isotopomers of a particular isotopologue, there would be equal probabilities for all bonding sites. As seen, when one deuterium atom is introduced, there is 76% probability that it will be found in position d or e and 17% probability that it will be found in position c. The preference is not surprising given the zero-point corrected energies at the stationary points for CH_4D^+, reported in Figure 2a. If the first deuterium atom is in position e, the second deuterium atom will be preferentially found in positions c or d, with nearly equal probability. When three deuterium atoms are present, they will be found in positions, a or c, d, and e. Finally, based in Figure 2b, we expect that when four deuterium atoms are present, the one remaining hydrogen atom will be found in position a or b. This is what is seen in the probabilities given in Table 2. Although not reported, similar trends were also seen when we investigated the effects of deuteration using the MP2-based potential surface of Brown, Braams and Bowman.[9] Such quantum localization has been seen in earlier studies by us[8,24] as well as in path integral Monte Carlo studies of Marx and Parrinello.[6]

Finally, in Table 1, we also report the zero-point energies of the isotopologues when ^{12}C is replaced by ^{13}C. These follow similar trends to the $^{12}CH_5^+$ and its deuterated isotopologues. Specifically, the substitution of ^{13}C for ^{12}C lowers the zero-point energy by a nearly constant amount of roughly 30 cm^{-1}.

Before moving on to a discussion of the nature of the ground-state wave functions, we note that several other studies have reported zero-point energy for CH_5^+ using DMC. Specifically, we reported zero-point energies for CH_5^+, $CH_2D_3^+$ and CD_5^+ based on an earlier MP2-based potential surface, and these, along with the zero-point energies for the other three isotopologues, are included in Table 1.[9] More recently, Jin et al. reported DMC zero-point energies for a global version of their CCSD(T) potential surface.[18] These zero-point energies were obtained by an approach that is similar to that used in the present study. As is seen in the results in Table 1, the zero-point energies differ by as much as 9 cm^{-1}. While the zero-point energies obtained from the global and nonglobal versions of the CCSD(T) surface of Jin, Braams and Bowman have overlapping uncertainties, the values that were obtained from the global surface are larger in all cases. These systematic differences reflect subtle differences between the global and nonglobal versions of this potential surfaces.

The differences between the present results and those obtained using a potential that was fit to electronic energies, obtained at the same configurations but at the MP2 level of theory, are somewhat larger (between 40 and 70 cm^{-1}).[8,9] The energies from the CCSD(T) surface are smaller. In the case of CH_5^+, a nearly identical zero-point energy was reported for the MP2 surface, using semiclassical, initial value representation calculations.[30]

The differences between the DMC zero-point energies that were reported based on the interpolated CCSD(T) based surface of Thompson et al. are larger.[10] In this case, they report a zero-point energy of 11095 (13) cm^{-1}, which is 187 cm^{-1} larger than the value we obtain from the CCSD(T) surface of Jin et al. This difference is surprising as both surfaces are based on electronic energies that were evaluated at the same level of theory, albeit with slightly different basis sets. In contrast, the method used to construct the surfaces from the electronic structure information is different. In addition, they used a smaller ensemble size for their DMC simulations than was used in the present investigations. We believe that both of these differences contribute to the disparity in zero-point energies.

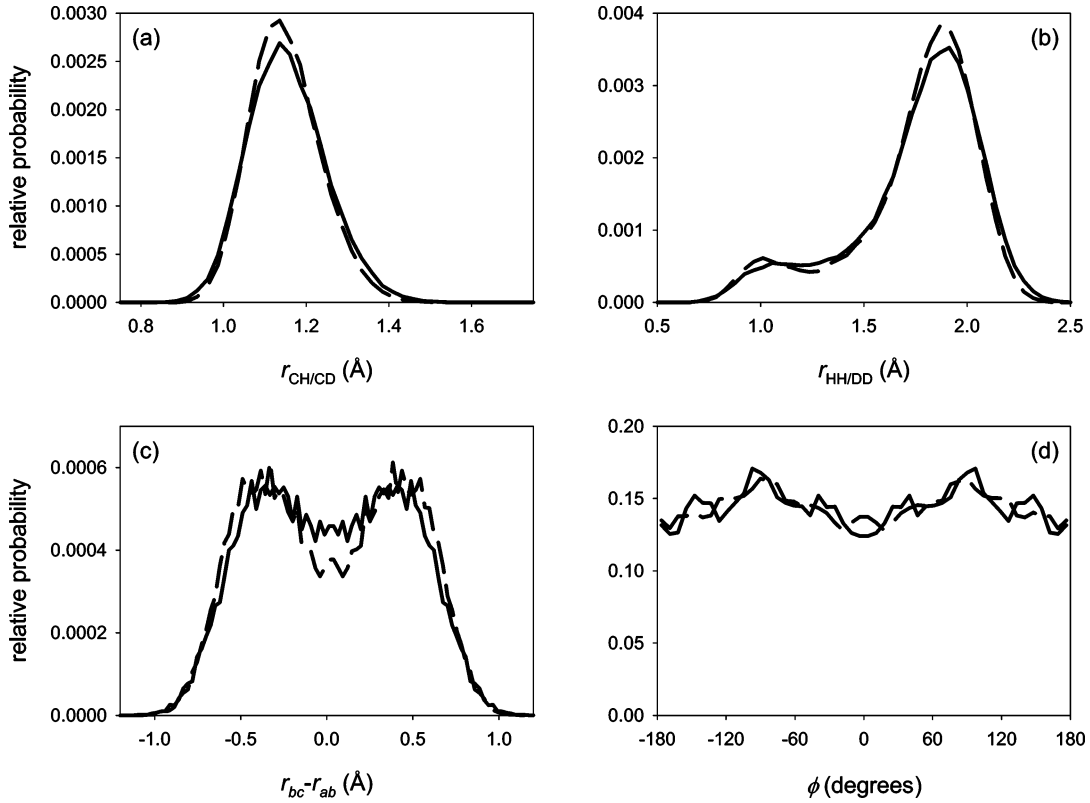

Figure 3. Projections of the ground-state wave functions for CH_5^+ (solid lines) and CD_5^+ (dashed lines) onto (a) the CH/D distances, (b) the HH/DD distances, (c) $r_{bc} - r_{ab}$, and (d) ϕ.

5.2. Probability Amplitudes. To further investigate the "structure" of CH_5^+ and its deuterated isotopologues, we plot projections of the ground-state wave function onto various internal coordinates. The results for CH_5^+ and CD_5^+ are plotted in Figure 3. These plots represent the average over all equivalent distances and the dispersion of the results for different specific hydrogen or deuterium atoms is roughly twice the width of the lines. These distributions are very similar to those reported in ref 9. The most notable difference is seen in the projection of the probability amplitudes onto $q = r_{bc} - r_{ab}$, the flipping motion of the H_b. The distribution obtained in the earlier work showed a single broad peak, centered at $q = 0$ whereas now there is a minimum in the distribution at this configuration. This difference reflects the fact that the C_{2v} saddle point is at 341 cm^{-1} on the CCSD(T) surface whereas its energy was only 193 cm^{-1} on the MP2 surface.

Focusing on the CH and HH distance distributions, we find that the distributions for CD_5^+ are slightly narrower than those for CH_5^+. This reflects the lowering in the zero-point energy upon deuteration. Interestingly, this narrowing is considerably smaller than the factor of $1/\sqrt{2}$ that one would expect if the central frequency of the CH stretch at all five bonding sites were equal. As has been discussed previously,[9] this reflects the fact that while CH_5^+ is highly fluxional along the two isomerization coordinates, on average the five hydrogen atoms are inequivalent, and the range of CH distances is well approximated by a weighted average of the CH distances in the C_s(I) minimum of CH_5^+, broadened by their harmonic zero-point probability amplitudes. A similar model can be used to understand the shape of the HH distance distributions, shown in Figure 3b. Here the distributions are bimodal, with the peak at 1 Å reflecting the distance between the hydrogen atoms in positions a and b at the C_s stationary points, while the larger peak is reflecting the nearly equal distances between the three hydrogen atoms in the CH_3^+ as well as the distances between the atoms in positions c and d and those in positions a and b. The slightly greater structure in the distribution for CD_5^+ reflects the increase in the effective height of the C_{2v} saddle point energy, thereby lowering the probability amplitude for $q = 0$, as is seen in Figure 3c. Finally, for both species the probability amplitude is completely delocalized in ϕ, with slightly larger probability amplitudes near the C_s(II) saddle point. This reflects the fact that once zero-point energy is considered, this configuration is somewhat lower in energy than the equilibrium structure.[19]

In Figure 4, we plot the distributions for CH_4D^+. As seen, the CD distances are, on average, shorter than the CH distances. Likewise, the peak at 1 Å in the HH distance distribution is dominated by the HH distance distribution with little contribution from the HD distribution. In panels c and d, we divide the distributions according to the positions of the deuterium atom, so that separate distributions are plotted for each possible bonding site of the deuterium in the C_s(I) minimum. While the labels on the atoms are defined so as to ensure that q is positive, we have continued each curve to negative values by switching the labels on atoms a and c. As is seen in the results reported in Table 2, the most probable position for the single deuterium atom is d or e, followed by position c. The distributions for these two bonding sites correspond to the solid and dashed lines in Figure 4c. The next lowest probability position for the hydrogen atom is position a, and this distribution is plotted with a dotted line. Since positions a and c are equivalent at the C_{2v} saddle point ($q = 0$) the dashed and dotted lines cross at $q = 0$.

Focusing on the projections of the probability distribution onto ϕ, we find that when two of the hydrogen atoms are in positions a and b, it is more probable that one of the remaining hydrogen atoms will be in position c. This leads to the peaks in the ϕ distribution for $|\phi| < 60°$ and $|\phi| > 120°$. This is consistent

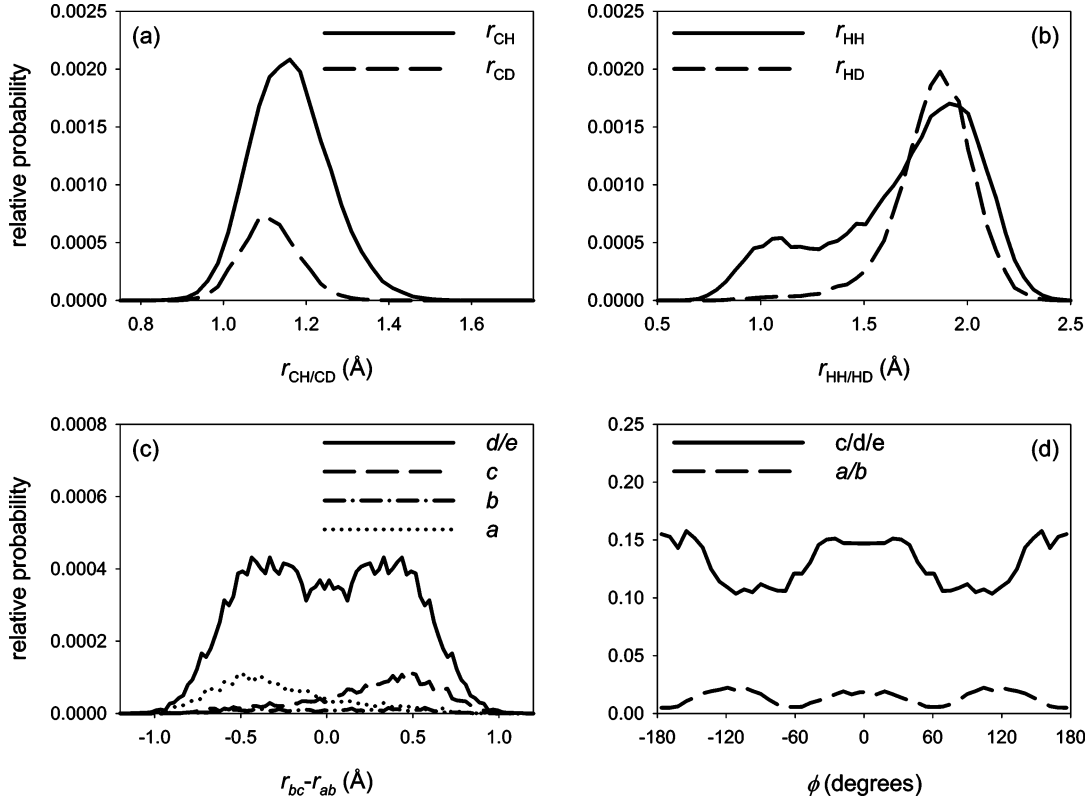

Figure 4. Same as Figure 3 for CH_4D^+. The definitions of the line-styles are given in the plots, where in panels c and d, the letter reflects the position of the deuterium atom.

with the propensity for the deuterium atom to be in position d or e for which the value of ϕ tends to be closer to 90 °. Finally, if the deuterium atom is in position a or b, it is more likely to be in position a than b. This is reflected in the greater probability for $\phi = 0$ or $\pm 120°$ than for $\phi = \pm 60$ or 180°. Similar distributions are seen for the other three mixed isotopologues. As with CH_4D^+, the shapes of the distributions can be easily rationalized in terms of the propensities for localization of the deuterium atoms into specific bonding sites.

5.3. Rotational Constants. Vibrationally averaged rotational constants are of particular interest for CH_5^+ and its deuterated analogues as low-temperature, rotationally resolved spectra are now being reported.[15] Experimentally derived rotational constants are based on fits of line positions and intensities to a model Hamiltonian that is based on the results of applying second-order perturbation theory to the full Hamiltonian. As such, it is not immediately obvious that this model should be appropriate for a system as fluxional as CH_5^+. Even for molecules that have more localized structure, it is not always clear what the appropriate functional form should be for the operators that correspond to rotational constants. Experimentally, the effects of resonant interactions, for example Coriolis couplings, are folded into these terms in the effective Hamiltonian.

As discussed above, we employ an Eckart embedding of the body-fixed axis system and, within this reference, obtain the expectation values of the elements of the inverse of the moment of inertia tensor. This approach is based on separation of rotational and so-called vibrational angular momentum for displacements from a reference geometry. In the case of CH_5^+, there are several possible choices for this reference geometry. In particular, all three of the stationary points on the potential, shown in Figure 1, could provide reasonable reference structures. Once one deuterium atom is introduced these three structures become ten, as there are four symmetry unique bonding sites in the C_s(I) minimum and three each for the C_s(II) and C_{2v} structures. When there are two deuterium atoms, this number increases to 18.

TABLE 3: Equilibrium and Vibrationally Averaged Rotational Constants for CH_5^+ and CD_5^+

CH_5^+	A_e	B_e	C_e	A	B	C
C_s(I)[a]	4.441	3.842	3.644	3.892(0.010)	3.861(0.010)	3.850(0.010)
C_s(II)	4.443	3.822	3.645	3.890(0.010)	3.864(0.010)	3.849(0.010)
C_{2v}	4.376	3.961	3.779	3.895(0.010)	3.867(0.010)	3.850(0.010)
CD_5^+	A_e	B_e	C_e	A	B	C
C_s(I)[a]	2.222	1.948	1.846	1.980(0.006)	1.964(0.006)	1.956(0.006)
C_s(II)	2.224	1.938	1.847	1.979(0.006)	1.965(0.006)	1.956(0.006)
C_{2v}	2.190	2.004	1.911	1.981(0.006)	1.966(0.006)	1.953(0.006)

[a] These equilibrium rotational constants differ from those that were obtained directly from a minimization at the CCSD(T)/aug-cc-pVTZ level of electronic structure theory/basis setby less than 0.001 cm^{-1}.[31]

The three equilibrium rotational constants for the three stationary points in CH_5^+ and CD_5^+ are reported in Table 3. As seen, the values of these constants depend on the stationary point that is used. In the case of CH_4D^+, the range of the equilibrium rotational constants is even larger. For example, the A constant ranges from 3.8 to 4.4 cm^{-1}, depending on which of the hydrogen atoms is replaced by a deuterium atom. On the other hand, as seen in Table 3, the rotational constants that we evaluate for CH_5^+ and CD_5^+, using the three stationary points on the potential as reference structures, differ by less than their statistical uncertainties. This relative insensitivity of the rotational constants to the choice of reference geometries gives us confidence that this approach will provide meaningful results, even for a species as fluxional as CH_5^+.

If we compare the values, obtained here with those reported by Thompson et al.[10] we find that the present values are larger by 0.06−0.08 cm^{-1}. This would reflect somewhat smaller

TABLE 4: Rotational Constants for the Isotopologues of CH_5^+ [a]

species	CH_4D^+	$CH_3D_2^+$	$CH_2D_3^+$	CHD_4^+
B_{aa}[b]	3.715	3.154	2.552	2.190
B_{bb}	3.093	2.800	2.550	2.175
B_{cc}	3.064	2.541	2.272	2.174
B_{ab}	0.146	0.022	0.002	0.002
B_{ac}	0.025	0.035	0.009	0.001
B_{bc}	0.010	0.047	0.039	0.007

[a] The results represent the average of many runs. Individual results and uncertainties are reported in the Supporting Information. [b] See eq 2.

average CH distances. When we compare the values reported for the C_s(I) minimum structure, given in Table 3, to the values reported in ref 10 [4.30, 3.93, and 3.62 cm^{-1}], we find that, on average, the values for the surface of Jin et al., used in the present study, are larger by 0.08 cm^{-1}. As such, we attribute the differences in the calculated rotational constants that are obtained from the two surfaces to differences in the minimum energy structures.

When we compare the rotational constants to those that were obtained from the earlier, MP2 surface, we find that the average values for the MP2 surface were 3.91 and 1.98 cm^{-1} for CH_5^+ and CD_5^+. On the CCSD(T) surface, they decrease to 3.87 and 1.97 cm^{-1}. This small decrease likely reflects the slightly smaller CH distances in the minimum energy geometry on the CCSD-(T) surface compared to that on the MP2 surface.

For the other isotopologues, we calculated the average rotational constants for each of the three stationary points, using the weighted average, based on the probability amplitude near each of the stationary points used to obtain the average spectra, discussed in ref 24. For each isotopologue, we averaged the rotational constants over 16 different replicas of the probability density. We enforced the invariance of the wave function by permuting all identical atoms in each of the walkers. In other words, for CH_5^+ or CD_5^+, each of the walkers was replaced by 120 walkers, while for the mixed isotoplogues they were replaced by 24 or 12 walkers. The statistical uncertainties in these calculations were less than 0.01 cm^{-1}. We then averaged the resulting rotational constants over the symmetry unique isotopomers of each of the stationary points geometries. The uncertainties, reported in Table S.3 of the Supporting Information, reflect the uncertainties in these quantities. In Table 4, we report the average of these quantities. The rotational constants, are given by $\hbar^2/2$ times the value of the elements of the inverse moment of inertia tensor, and the effective rotational Hamiltonian is defined as

$$\hat{H}_{\mathrm{rot}} = B_{aa}\hat{J}_a^2 + B_{bb}\hat{J}_b^2 + B_{ab}[\hat{J}_a\hat{J}_b + \hat{J}_b\hat{J}_a] + B_{cc}\hat{J}_b^2 + B_{ac}[\hat{J}_a\hat{J}_c + \hat{J}_c\hat{J}_a] + B_{bc}[\hat{J}_b\hat{J}_c + \hat{J}_c\hat{J}_b] \quad (2)$$

As is seen, in most cases, the off-diagonal elements are zero, or nearly zero.

6. Spectra

Before concluding, we consider the vibrational spectra for the various isotopologues of CH_5^+. We recently reported low-resolution calculated spectra for CH_5^+, CH_4D^+, CHD_4^+, and CD_5^+.[15,24] Here we present the calculated spectra for the remaining two species in this series. The basic idea for all of these calculations is to first evaluate the probability amplitudes for each of the isotopomers of each of the isotopologues near the three stationary points. In the case of $CH_2D_3^+$ and $CH_3D_2^+$, there are seven symmetry unique arrangements of the two hydrogen or deuterium atoms at the C_s(I) minimum. At the C_{2v} configuration, there are five and there are six at the C_s(II) configuration. The relative probability amplitudes in the vicinity of these stationary points are reported in the Supporting Information. To obtain the spectra, plotted in thick solid and dashed lines in Figure 5a, we convolute the harmonic spectra, evaluated at each of the stationary points by a Gaussian with a full-width at half-maximum of 200 cm^{-1}. For comparison, we have also plotted the spectra for the remaining four isotopologues with thin lines. These spectra are identical to those reported in ref 24. Likewise, we have plotted the convolution of the VCI spectra that were calculated by Huang and Bowman,[32] using their program MULTIMODE.[23] The spectra that are plotted in Figure 5b represent weighted averages of the spectra calculated using each of the stationary points of all isotopomers for which the relative population is larger than 0.15 as reference geometries for the normal mode basis in the VCI calculations. Details of the VCI calculations for CH_5^+ can be found elsewhere.[15,24]

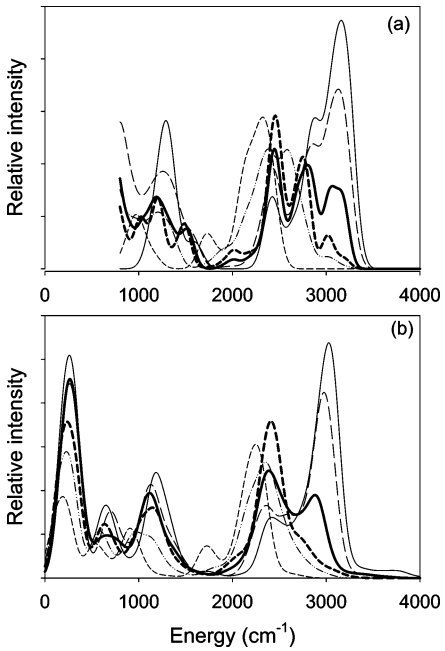

Figure 5. Plots of the (a) harmonic and (b) VCI[32] spectra for $CH_2D_3^+$ (thick dashed line) and $CH_3D_2^+$ (thick solid line) in the CH/D stretch and bend regions. For comparison, the spectra for the other four isotopologues have are plotted here [CH_5^+ (thin solid line), CH_4D^+ (thin long-dashed line), CHD_4^+ (thin dot-dot−dashed line) and CD_5^+ (thin short dashed line)].

In CH_5^+, it is expected that the harmonic approximation will be most valid in the CH stretch and HCH bend regions of the spectrum, above roughly 800 cm^{-1}. It will not be appropriate at lower frequencies as the low-frequency modes are very anharmonic. Consequently the harmonic spectra are plotted for frequencies above 800 cm^{-1}.

Comparing the six spectra plotted in Figure 5, there are several interesting trends. To start we focus on the CH/D stretch region which is above 2400 cm^{-1} for the CH stretches, 1500 cm^{-1} for the CD stretches. On the blue side of these bands, we find a distinct red-shift and a decrease in intensity. The origins of this can be easily seen by looking at the highest frequency CH stretches in Table 1. Specifically, it is most likely that the deuterium atoms will be found in the bonding sites that correspond to the highest CH stretch frequencies. This leads to the loss in intensity on the blue side of the CH stretch band as CH_5^+ is partially deuterated. In contrast, if we focus on the part

of the band near 2300−2400 cm^{-1}, we find that its position and width are roughly the same when there are two to five hydrogen atoms, although the intensity increases with increasing number of deuterium atoms. This reflects the fact that the lowest frequency CH stretch and the highest frequency CD stretch modes are both at roughly this frequency, as is seen in Table 1. It is interesting to note that the CH/D stretch bands in $CH_3D_2^+$ and the $CH_2D_3^+$ spectra span roughly the same frequency ranges, and their profiles are very similar between 1700 and 2900 cm^{-1} in the harmonic spectra, 1800−2700 cm^{-1} in the VCI spectra. This reflects the fact that the transitions associated with the CH stretches tend to be more intense than those associated with the CD stretches, and the hydrogen atoms in these two species tend to occupy the same bonding sites, as is shown in Table 2. Similar trends are also seen in the HCH bend peak in the spectra.

Finally, we focus on the large peaks at roughly 200 cm^{-1} in the VCI spectra in Figure 5b. We note that the frequency and the width of these peaks are roughly the same for all but the CD_5^+ spectrum. This feature has been assigned to the fundamental in the flip vibration.[15] Comparing this frequency to those reported in Table 1, the anharmonic frequency is considerably lower than the harmonic ones. This should not be surprising based on projections of the ground-state probability amplitude onto this coordinate, plotted in Figure 3c. Despite this, the trends in the frequency of this mode for the six isotopologues are consistent with the spectrum.

Before concluding this section, there are two important things to note about the differences between the harmonic and VCI spectra. First, the harmonic spectra have not been scaled. The unscaled frequencies were used because the appropriate scaling will depend on the anharmonicity of the mode, and the breadth of the CH/D stretch region provides a clue that the scaling factors will not be the same for all of the CH stretches. In addition, since we only consider transitions to the fundamentals, structures are often seen in the harmonic spectra at this level of resolution that will be washed out when a fully coupled, anharmonic treatment is applied. As a result, the spectra in Figure 5a show more structure than those in Figure 5b.

7. Summary and Conclusions

In this paper, we have presented the results of an investigation of the ground-state properties of CH_5^+ and its deuterated analogues. These calculations are based on fully ab initio potential and dipole moment surfaces.[9,18] In the first part of the paper, we quantified the extent of localization of the vibrational ground states. These results are consistent with earlier studies[9] and demonstrate that, while CH_5^+ and CD_5^+ are completely delocalized along the two isomerization coordinates, ϕ and q, signatures of their minimum energy structure can be seen in the CH and HH probability distributions.

In the second part of the paper, we investigated the implications of the large amplitude motions on spectroscopically measurable quantities, specifically the rotational constants and the vibrational frequencies and intensities, particularly in the CH/CD stretch region. Somewhat surprisingly, the rotational constants, evaluated within an Eckart frame, appear to be robust quantities insofar as their values were found to be relatively insensitive to the reference geometries used to evaluate them. Finally, we investigated trends in the spectra upon deuteration. The localization of the deuterium atoms makes the transition from CH_5^+ to CD_5^+ less smooth than one might expect, reflecting differences in intensities of different CH/D stretch bands.

As is indicated in the Introduction, CH_5^+, with its five hydrogen atoms bonded to a single carbon atom, represents an unusual species that is expected to undergo large amplitude motions, even in its ground vibrational state. Over the coming years, it is anticipated that significant advances will be made in assigning the experimental spectra, and as we continue to probe the spectroscopy and dynamics of this unusual system, it is likely that further surprising features will be observed.

Acknowledgment. Support through grants from the Chemistry Division of the National Science Foundation is gratefully acknowledged. We also thank Professor Joel M. Bowman for many discussions on these systems and for providing us with the codes used to evaluate the potential and dipole moment surfaces used in this work as well as their calculated VCI spectra that are included in Figure 5.

Supporting Information Available: Table giving weights used to obtain the averaged rotational constants for the mixed isotopologues of CH_5^+ as well as the spectra for $CH_3D_2^+$ and $CH_2D_3^+$ and rotational constants evaluated using different reference geometries. This material is available free of charge via the Internet at http://pubs.acs.org.

References and Notes

(1) Herbst, E. *J. Phys. Chem. A* **2005**, *109*, 4017.
(2) Olah, A.; Rasul, G. *Acc. Chem. Res.* **1997**, *30*, 245.
(3) Brown, A.; Braams, B. J.; Christoffel, K.; Jin, Z.; Bowman, J. M. *J. Chem. Phys.* **2003**, *119*, 8790.
(4) Marx, D.; Parrinello, M. *Nature (London)* **1995**, *375*, 216.
(5) Marx, D.; Parrinello, M. *Z. Phys. D* **1997**, *41*, 253.
(6) Marx, D.; Parrinello, M. *Science* **1999**, *286*, 1051.
(7) Kumar P, P.; Marx, D. *Phys. Chem./Chem. Phys.* **2006**, *8*, 573.
(8) McCoy, A. B.; Braams, B. J.; Brown, A.; Huang, X.; Jin, Z.; Bowman, J. M. *J. Phys. Chem. A* **2004**, *108*, 4991.
(9) Brown, A.; McCoy, A. B.; Braams, B. J.; Jin, Z.; Bowman, J. M. *J. Chem. Phys.* **2004**, *121*, 4105.
(10) Thompson, K. C.; Crittenden, D. L.; Jordan, M. J. T. *J. Am. Chem. Soc.* **2005**, *127*, 4954.
(11) East, A. L. L.; Kolbuszewski, M.; Bunker, P. R. *J. Phys. Chem. A* **1997**, *101*, 6746.
(12) Kolbuszewski, M.; Bunker, P. R. *J. Chem. Phys.* **1996**, *105*, 3649.
(13) Bunker, P. R.; Ostojic, B.; Yurchenko, S. *J. Mol. Struct.* **2004**, *695*, 253.
(14) White, E. T.; Tang, J.; Oka, T. *Science* **1999**, *284*, 135.
(15) Huang, X.; McCoy, A. B.; Bowman, J. M.; Johnson, L. M.; Savage, C.; Dong, F.; Nesbitt, D. J. *Science* **2006**, *311*, 60.
(16) Komornicki, A.; Dixon, D. A. *J. Chem. Phys.* **1987**, *86*, 5625.
(17) Schreiner, P. R.; Kim, S. J.; Schaefer, H. F.; Schleyer, P. v. R. *J. Chem. Phys.* **1993**, *99*, 3716.
(18) Jin, Z.; Braams, B. J.; Bowman, J. M. *J. Phys. Chem. A* **2006**, *110*, 1569.
(19) McCoy, A. B. *Int. Rev. Phys. Chem.*, in press.
(20) Boo, D. W.; Liu, Z. F.; Suits, A. G.; Tse, J. S.; Lee, Y. T. *Science* **1995**, *269*, 57.
(21) Boo, D. W.; Lee, Y. T. *J. Chem. Phys.* **1995**, *103*, 520.
(22) Heck, A. J. R.; de Koning, L. J.; Nibbering, N. M. M. *J. Am. Soc. Mass Spectrom.* **1991**, *2*, 453.
(23) Bowman, J. M.; Carter, S.; Huang, X. C. *Int. Rev. Phys. Chem.* **2003**, *22*, 533.
(24) Huang, X.; Johnson, L. M.; Bowman, J. M.; McCoy, A. B. *J. Am. Chem. Soc.* **2006**, *128*, 3478.
(25) Anderson, J. B. *J. Chem. Phys.* **1976**, *65*, 4121.
(26) Suhm, M. A.; Watts, R. O. *Phys. Rep.* **1991**, *204*, 293.
(27) Langfelder, P.; Rothstein, S. M.; Vrbik, J. *J. Chem. Phys.* **1997**, *107*, 8526.
(28) Asvany, O.; Kumar, P.; Redlich, B.; Hegeman, I.; Schlemmer, S.; Marx, D. *Science* **2005**, *309*, 1219.
(29) Louck, J. D.; Galbraith, H. W. *Rev. Mod. Phys.* **1976**, *48*, 69.
(30) Kaledin, A. L.; Kunikeev, S. D.; Taylor, H. S. *J. Phys. Chem. A* **2004**, *108*, 4995.
(31) Jin, Z.; Bowman, J. M. Private communication.
(32) Huang, X.; Bowman, J. M. Private communication.